

Dilepton yields from Brown-Rho scaled vector mesons including memory effects

Björn Schenke and Carsten Greiner

*Institut für Theoretische Physik, Johann Wolfgang Goethe – Universität Frankfurt,
Max-von-Laue-Straße 1, D-60438 Frankfurt am Main, Germany*

Brown-Rho scaling, which has been strongly discussed after recent NA60 data was presented, is investigated within a nonequilibrium field theoretical description that includes quantum mechanical memory. Dimuon yields are calculated by application of a model for the fireball, and strong modifications are found in the comparison to quasi-equilibrium calculations, which assume instantaneous adjustment of all meson properties to the surrounding medium. In addition, we show results for the situation of very broad excitations.

PACS numbers: 11.10.Wx;05.70.Ln;25.75.-q

Motivated by the recent discussion on whether Brown-Rho scaling [1] is ‘ruled out’ by the NA60 data, presented at Quark Matter 2005 [2, 3], we calculate dilepton yields from ρ -mesons with dropping masses within the nonequilibrium quantum field formulation introduced in [4]. First quantitative but simplified calculations within this work have shown that memory effects, which are neglected in quasi-equilibrium calculations [5] and [6, 7, 8, 9], have an important influence on the final dilepton yields, especially for dropping mass scenarios. This lead to the conclusion that an analysis of which scenario describes the data correctly demands the proper inclusion of memory effects. The aim of this work is to clarify how the inclusion of memory affects the dimuon yields from Brown-Rho scaled vector mesons. The validity of standard equilibrium calculations depends on the strength of these effects.

We consider two mass parameterizations: The temperature and density dependent one used by Rapp et al. [10]

$$m_\rho^* = m_\rho(1 - 0.15 n_B/n_0) [1 - (T/T_c)^2]^{0.3}, \quad (1)$$

assuming a constant gauge coupling g in the vector meson dominance (VMD) -coupling, and one motivated by the renewed version of Brown-Rho scaling discussed in [11, 12]:

$$m_\rho^* = m_\rho(1 - 0.15 n_B/n_0), \quad (2)$$

with a modified gauge coupling g^* , in such a way that g^* is constant up to normal nuclear density n_0 , while from then on m_ρ^*/g^* is taken to be constant [13]. This parameterization is not valid close to T_c because it does not take the meson mass to zero at the critical point. However, Brown and Rho argue [11, 12] that because lattice calculations show that the pole mass of the vector mesons does not change appreciably up to $T = 125$ MeV, the parameterization using $[1 - (T/T_c)^n]^d$ (with positive d and integer n) overestimates the mass shift. They find temperature dependent effects to be an order of magnitude smaller than the density dependent effects, and hence suggest to concentrate on the density dependent part.

We also wish to study the effect of finite memory for a mass shift following this parameterization and ignore its shortcomings for the moment. Furthermore, Brown and Rho point out that due to the violation of VMD, which accounts for most of the shape of the dilepton spectrum (see [11, 12] and [14]), the overall dilepton production in dense matter should be reduced by a factor of 4 compared to Rapp’s calculations, which we do not take into account here.

We compare the usual approach [18], where the dilepton rate is given by the well known equilibrium formula

$$\frac{dN}{d^4x d^4k}(\tau, k) = \frac{2e^4}{(2\pi)^5} \frac{m_\rho^4}{g_\rho^2} \mathcal{L}(M) \times \frac{1}{M^2} n_B(T(\tau), k_0) \pi A_\rho(\tau, k), \quad (3)$$

with invariant mass $M^2 = k^2 = k_0^2 - \mathbf{k}^2$ and $\mathcal{L}(M) = \left(1 + \frac{2m_\rho^2}{M^2}\right) \sqrt{1 - \frac{4m_\rho^2}{M^2}} \theta(M^2 - 4m_\rho^2)$, to the nonequilibrium formalism, in which the propagators of the ρ -meson and the virtual photon are calculated using the general nonequilibrium formulas. The dilepton rate for a spatially homogeneous but time dependent system is given by [4]:

$$\frac{dN}{d^4x d^4k}(\tau, k) = \frac{2e^2}{(2\pi)^5} M^2 \mathcal{L}(M) \times \Re \left[\int_{t_0}^{\tau} d\bar{t} i D_{\gamma T}^<(\mathbf{k}, \tau, \bar{t}) e^{ik_0(\tau - \bar{t})} \right]. \quad (4)$$

In its derivation we treated transverse and longitudinal modes equally, which is adequate for our purposes. $D_{\gamma T}^<$ is the transverse virtual photon propagator, and satisfies the generalized fluctuation dissipation relation

$$D^< = D^{\text{ret}} q^< D^{\text{adv}}, \quad (5)$$

with all time variables and integrations, and further indices implicit. The relation follows directly from the Kadanoff-Baym equations when terms corresponding to initial conditions at time t_0 are omitted. This can be done when the system is given enough time to reach its initial

state before we start the actual calculation of the yield [4]. In this case the $D^{\text{ret/adv}}$ are the free retarded and advanced virtual photon propagators while $q^< = \Pi^<$, the photon self energy, follows VMD by

$$\Pi_T^<(t_1, t_2) = e^2 \frac{m_\rho^{*2}(t_1)}{g_\rho^*(t_1)} D_{\rho T}^<(t_1, t_2) \frac{m_\rho^{*2}(t_2)}{g_\rho^*(t_2)}. \quad (6)$$

Note that the couplings are to be taken at the correct vertices, separated in time. The free photon propagator has to be exponentially damped in order to reduce large contributions from early times, which make the extraction of the higher frequency structure numerically problematic [19].

The meson propagator $D_{\rho T}^<$ also satisfies (5), with $q^< = \Sigma^<$, the meson self energy, and the retarded and advanced meson propagators, which obey the equation of motion that in a spatially homogeneous and isotropic medium is given by

$$\begin{aligned} & (-\partial_{t_1}^2 - m_\rho^{*2} - \mathbf{k}^2) D_{\rho T}^{\text{ret}}(\mathbf{k}, t_1, t_2) \\ & - \int_{t_2}^{t_1} d\bar{t} \Sigma_{\rho T}^{\text{ret}}(\mathbf{k}, t_1, \bar{t}) D_{\rho T}^{\text{ret}}(\mathbf{k}, \bar{t}, t_2) = \delta(t_1 - t_2), \end{aligned} \quad (7)$$

and $D_{\rho T}^{\text{adv}}(\mathbf{k}, t_1, t_2) = D_{\rho T}^{\text{ret}}(\mathbf{k}, t_2, t_1)$. For calculating $\Sigma^<$ from Σ^{ret} we assume local equilibrium and introduce the fireball temperature to the calculation. The integral over past times in Eq. (4) as well as the time integrations in Eq. (5) have encoded the finite memory of the system. In [4] we show that in order to describe a heavy ion reaction it is essential to retain this dynamic information. This is due to the time scales for the adaption of the meson's spectral properties to the evolving medium being of the same order as the lifetime of the regarded hadronic system. In this situation the evolution is non-Markovian and quantum mechanical interferences among past time contributions become important [4]. Therefore a gradient approximation can not properly describe the situation in a heavy ion collision and remarkable differences between the dynamic and the Markovian yields occur.

Following [7, 8, 15], we use a fireball model with a cylindrical volume expansion in the $\pm z$ direction:

$$V(\tau) = (z_0 + v_z \tau) \pi (r_0 + 0.5 a_\perp \tau^2)^2, \quad (8)$$

where z_0 is equivalent to a formation time, $v_z = c$ is the primordial longitudinal motion, $r_0 = 5.15$ fm is the initial nuclear overlap radius, and $a_\perp = 0.08 c^2/\text{fm}$ is the radial acceleration. We start the calculation at $T = T_c = 175$ MeV (at $\tau_0 \approx 3$ fm/c) and set the meson self energy $\Sigma^<$ to zero for temperatures below chemical freezeout at $T = 120$ MeV, thus ending the production of ρ -mesons. The hadronic phase, for which we calculate the dimuon production, lives for about 6 fm/c. The time dependent temperature and density, determined via the fireball evolution, yield the time dependence of the ρ -meson mass

following parameterizations (1) and (2). We include additional broadening by about 100 MeV as it was done in Rapp's calculation [10] shown in [3]. In the dynamic case the ρ -meson propagator and the photon propagator follow Eq. (5) after a Fourier transformation of the self energy into the two time representation. The rate is then calculated using Eq. (4), whereas in the quasi-equilibrium case the rate at a certain time follows directly from Eq. (3), using the spectral function and Bose-distribution corresponding to the present mass and temperature. The calculation is done for each momentum mode between $k = 0$ and $k = 1.5$ GeV and integrated over momenta. We show the comparison of the dynamic and the quasi-equilibrium calculation for the two parameterizations in Figs. 1 and 2. We find a strong enhance-

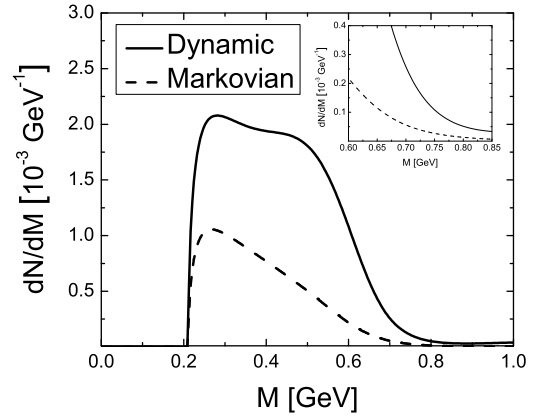


FIG. 1: Dimuon yield from decaying ρ -mesons calculated out of equilibrium and within the usual static approximation using parameterization (1). A difference of about a factor of 4 is visible in the regime between 400 and 800 MeV.

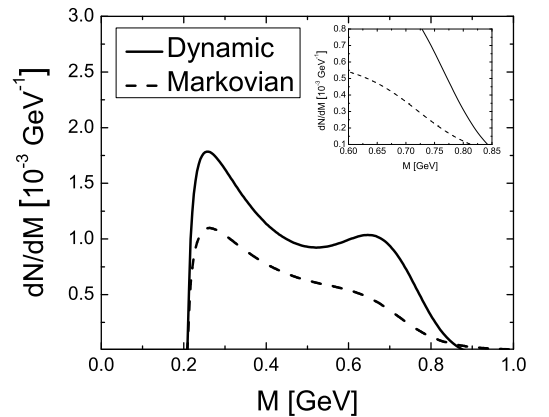


FIG. 2: Dimuon yield from decaying ρ -mesons calculated out of equilibrium and within the usual static approximation using parameterization (2). The most significant difference (about a factor of 2-3) is visible between 600 and 800 MeV.

ment as well as modification of shape in both cases. For

the density and temperature dependent parameterization the dynamic calculation yields about a factor of 4 more dileptons between invariant masses of 400 and 800 MeV as compared to the Markovian case, while the other parameterization shows an enhancement of about 2-3 times between 600 and 800 MeV in the dynamic calculation.

The reasons for the strong differences are the following: First, the meson mass effectively approaches its vacuum value more slowly in the dynamic calculation. Lower masses are enhanced due to the Bose factor and if the spectral function has a lower mass for a longer time enhancement is greater. Second, the memory of higher temperatures increases this enhancement for all masses. Finally, the modified coupling in Eq. (6) suppresses the early contributions. This means that for the static case all low masses in the spectral function and high temperatures are suppressed. However, due to the finite memory in the dynamic case, these low masses and high temperatures still contribute at later times when the coupling is larger, meaning that they are less suppressed by the VMD-coupling.

In the first case, besides the overall increase in yield, we find a significant enhancement in the dynamic calculation for invariant masses around the ρ -vacuum mass. Comparing to NA60 data (shown vs. the equilibrium Brown-Rho calculation in e.g. [3, 11]), the enhancement would improve the situation for the Brown-Rho scenario, which in the equilibrium calculation strongly underestimates the data in this regime. The second parameterization leads to even more weight around the vacuum peak in the dynamic case and would also improve the agreement with the data.

Having investigated pure dropping mass scenarios, we now combine Brown-Rho-scaling using parameterization (1) with strong broadening and coupling to the excitation $N^*(1520)$. This is achieved by using the self energy [4]

$$\text{Im}\Sigma^{\text{ret}}(\tau, \omega, \mathbf{k}) = -\frac{\rho(\tau)}{3} \left(\frac{f_{RN\rho}}{m_\rho} \right)^2 \times g_I \frac{\omega^3 \bar{E} \Gamma_R(\tau)}{(\omega^2 - \frac{\Gamma_R(\tau)^2}{4} - \bar{E}^2)^2 + (\Gamma_R(\tau)\omega)^2} - \omega\Gamma(\tau), \quad (9)$$

with $\bar{E} = \sqrt{m_R^2 + \mathbf{k}^2} - m_N$ and m_R and m_N the masses of the resonance and nucleon, respectively [16]. Γ_R is the width of the resonance, which in vacuum is 120 MeV, and g_I the isospin factor. Both widths Γ and Γ_R increase substantially in the medium ($\Gamma \rightarrow 700$ MeV and $\Gamma_R \rightarrow 400$ MeV) [7, 17]. The transverse and longitudinal components of the self energy (9) have been combined, following our approximation of treating both contributions equally. Note that we are always using the vacuum ρ -mass in Eq. (9) to prevent the coupling to the resonance from becoming infinite. Typical resulting spectral functions are shown in Fig. 3.

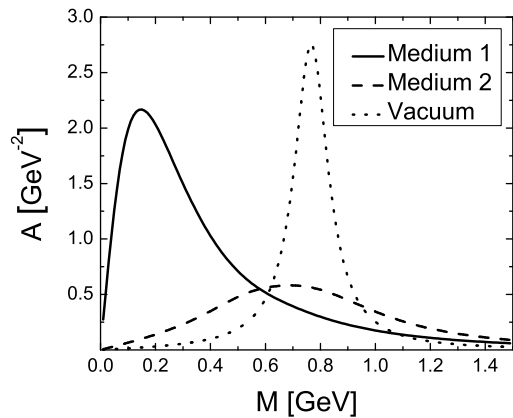


FIG. 3: Medium modified spectral function using self energy (9) with (Medium 1: $m = 300$ MeV) and without (Medium 2) mass shift at normal nuclear density and widths of $\Gamma = 700$ MeV and $\Gamma_R = 400$ MeV. The ρ -vacuum spectral function is shown for comparison.

The result of the calculation combining Brown-Rho scaling, broadening and coupling to the $N^*(1520)$ is presented in Fig. 4. Here, the differences between the Markovian and the dynamic calculations seem less significant as compared to the mass shift scenarios with only marginal broadening (cf. Figs. 1 and 2). This can be expected since the memory time scales approximately with the inverse width in the system (see [4]). The very broad spectral function adjusts faster to the medium changes. However, around the ρ -vacuum mass the dynamic calculation still leads to around three times more yield than the Markovian one.

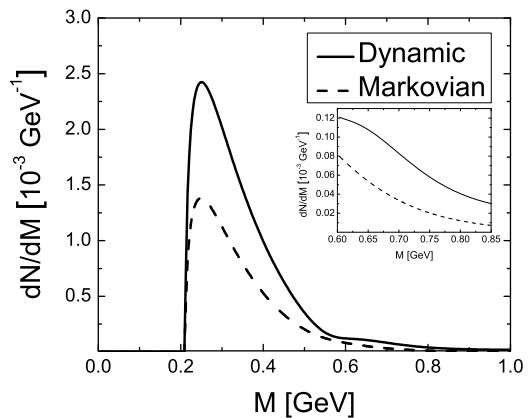


FIG. 4: Dimuon yield from decaying ρ -mesons calculated out of equilibrium and within the Markovian approximation using parameterization (1) for the meson mass and coupling to the $N^*(1520)$ resonance by means of the self energy (9).

For comparison we present the calculation for a scenario with coupling to the resonance and broadening but without dropping mass (Fig. 5). The major difference to

the scenario with dropping mass is the overall increase of the yield. This is due to the fact that in the dropping mass case, spectral weight is shifted below the threshold of twice the muon mass at early times. For the case without mass shift the difference between the dynamic and Markovian calculations is less than 30% for an invariant mass up to 650 MeV (above that differences reach about 50%). This is again due to the very broad spectral function, for that memory effects become less significant. Furthermore, the time scale for adjustment to the medium [4] also depends on the pole mass of the spectral function. Lower masses mean larger memory times, such that for dropping mass scenarios the effects are naturally larger.

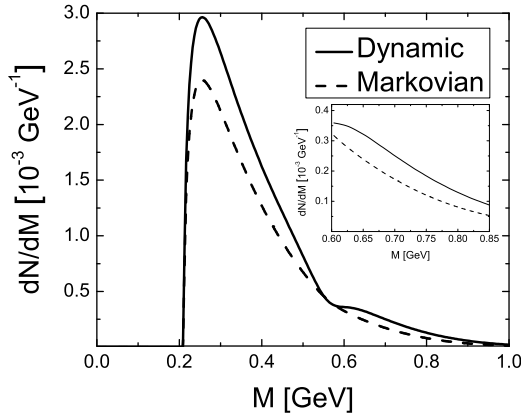


FIG. 5: Dimuon yield from decaying ρ -mesons calculated out of equilibrium and within the Markovian approximation using coupling to the $N^*(1520)$ and broadening of both the vacuum and the resonance peak to 400 MeV. Maximal differences between the two calculations are about 30%.

In summary, we have shown that the inclusion of finite memory by calculation of the dilepton yield within a nonequilibrium field theoretical setup, using the realtime formalism, yields moderate to strong differences when comparing to dilepton yields, calculated assuming instantaneous adaption of all meson properties to the medium. Particularly, we have compared the results for dropping mass scenarios for dimuon yields in the NA60 scenario, which is modelled by an expanding fireball. An enhancement by about a factor of 3-4 around the ρ -vacuum mass and significant differences in shape have been found for the case of dropping mass with moderate broadening by 100 MeV. Inclusion of coupling to the $N^*(1520)$ resonance and significant broadening strongly modifies the shape of the calculated yields, especially in the dynamic calculation. However, the yield is still enhanced and more weight lies around the ρ -vacuum mass in the dynamic calculation. This is important for the comparison to the NA60 data, where the Markovian calculation us-

ing Brown-Rho scaling lead to too few dimuons in that region [3, 11]. A scenario without mass shifts but including strong broadening [7] is less affected by the inclusion of memory. The dynamic calculation differs from the Markovian one by maximally 50%, and less than 30% in most of the regarded range.

We conclude that memory effects must not be neglected in precision calculations of dilepton yields from relativistic heavy ion collisions. Every dropping mass scenario we have investigated shows a significant dependence on whether instantaneous adaption to the medium or the full quantum mechanical evolution are considered.

Acknowledgments

B.S. thanks G.E. Brown and R. Rapp for stimulating discussions.

-
- [1] G. E. Brown and M. Rho, Phys. Rev. Lett. **66**, 2720 (1991).
 - [2] S. Damjanovic et al. (NA60) (2005), nucl-ex/0510044.
 - [3] R. Arnaldi et al. (NA60), Phys. Rev. Lett. **96**, 162302 (2006), nucl-ex/0605007.
 - [4] B. Schenke and C. Greiner, Phys. Rev. **C73**, 034909 (2006), hep-ph/0509026.
 - [5] R. Rapp and J. Wambach, Adv. Nucl. Phys. **25**, 1 (2000), hep-ph/9909229.
 - [6] V. V. Skokov and V. D. Toneev (2005), nucl-th/0509085.
 - [7] H. van Hees and R. Rapp (2006), hep-ph/0603084.
 - [8] H. van Hees and R. Rapp (2006), hep-ph/0604269.
 - [9] T. Renk and J. Ruppert (2006), hep-ph/0605130.
 - [10] R. Rapp, private communication (2005).
 - [11] G. E. Brown and M. Rho (2005), nucl-th/0509001.
 - [12] G. E. Brown and M. Rho (2005), nucl-th/0509002.
 - [13] G. E. Brown and M. Rho, Phys. Rept. **398**, 301 (2004), nucl-th/0206021.
 - [14] M. Harada and K. Yamawaki, Phys. Rept. **381**, 1 (2003), hep-ph/0302103.
 - [15] R. Rapp and J. Wambach, Eur. Phys. J. **A6**, 415 (1999), hep-ph/9907502.
 - [16] M. Post, S. Leupold, and U. Mosel, Nucl. Phys. **A741**, 81 (2004), nucl-th/0309085.
 - [17] R. Rapp, M. Urban, M. Buballa, and J. Wambach, Phys. Lett. **B417**, 1 (1998), nucl-th/9709008.
 - [18] We will refer to this as the Markovian approach, because memory is completely neglected.
 - [19] Explicitly, we use the replacement $D_{\gamma T}^{\text{ret}}(\tau - t_1) = (\tau - t_1) \rightarrow (\tau - t_1)e^{-\Lambda(\tau - t_1)}$ and an analogous one for the advanced propagator. Then we renormalize the result by multiplication with $(\omega^2 + \Lambda^2)^2/\omega^4$ (see [4] for more details). Note that a variation of Λ between 200 and 800 MeV leads to a change in the resulting yield of up to 5% in the interesting region between 0.4 and 0.8 GeV. Differences very close to twice the muon mass reach about 15%.